

RESEARCH ARTICLE

# Comparison Performance Analysis of PI and PI-ANFIS in VSC-HVDC Transmission Systems

Muhamad Abdul Aziz and Faiz Husnayain\*

Department of Electrical Engineering, Faculty of Engineering, Universitas Indonesia, Depok, Indonesia

\*Corresponding author. Email: [faiz.h@ui.ac.id](mailto:faiz.h@ui.ac.id)

## Abstract

Voltage Source Converter–High Voltage Direct Current (VSC–HVDC) transmission systems are preferred for long–distance power transmission due to their flexibility and stability. However, maintaining optimal performance and stability during transient conditions and disturbances is challenging. This research analyzes the performance of VSC–HVDC systems using Proportional–Integral Adaptive Neuro–Fuzzy Inference System (PI–ANFIS) control compared to conventional PI control. A VSC–HVDC system model with PI control provides the basis for generating input–output data to train the ANFIS model. Subsequently, a VSC–HVDC model with PI–ANFIS control is developed and optimized. Performance evaluation under transient conditions and both permanent and temporary disturbances reveals that PI–ANFIS significantly enhances system performance. PI–ANFIS reduces overshoot, accelerates settling time in active power, reactive power, and DC voltage control, and improves stability and recovery time during disturbances. The adaptability and learning capabilities of ANFIS offer additional flexibility for dynamic conditions and unexpected disturbances. This study highlights intelligent control technology advancements, promoting reliable and adaptable power transmission systems, and lays the groundwork for future research and practical applications of PI–ANFIS control in VSC–HVDC systems.

**Keywords:** adaptability, disturbances, performance, PI–ANFIS control, power transmission systems, system stability, transient, VSC–HVDC

## 1. Introduction

High–Voltage Direct Current (HVDC) is an increasingly popular power transmission technology due to its ability to transmit power over long distances with minimal losses. One type of HVDC is Voltage Source Converter (VSC), which uses transistors

such as Insulated Gate Bipolar Transistors (IGBT) to convert alternating current (AC) to direct current (DC) and vice versa [1]. VSC-HVDC technology has several advantages compared to Line Commutated Converter (LCC)-HVDC, such as the ability to connect weak AC networks and provide independent control of active and reactive power [2].

VSC-HVDC is used in various applications due to its flexibility and ability to integrate renewable energy. One of the main applications is the integration of renewable energy, where VSC-HVDC allows large-scale integration of renewable energy sources such as wind and solar farms into the power grid. Projects in Denmark and China have successfully used VSC-HVDC to transmit power from offshore wind farms to the main power grid [1]. Another example is the reinforcement of urban networks, where VSC-HVDC can be used to connect urban load zones, improving the stability and reliability of electricity supply in densely populated areas [1]. In addition, VSC-HVDC also has the ability to assist in the black start process, where a power grid that has experienced a total blackout can be restarted without requiring operating power plants, which is very important in improving the resilience and reliability of the power system [3],[4].

Case studies highlighting the application of VSC-HVDC include the Gotland project in Sweden and the Nan'ao multi-terminal project in China. Both projects demonstrate how VSC-HVDC can be used to support the integration of renewable energy and improve the stability of local power grids. The Gotland project, for example, is the world's first commercial VSC-HVDC system used to transmit electricity from the island of Gotland to mainland Sweden, providing the dynamic reactive power support required by wind farms and improving the stability of the connected AC system [1]. The Nan'ao multi-terminal project in China is the world's first commercial multi-terminal VSC-HVDC project, designed to distribute power from multiple wind farms to the main grid and maintain power supply on Nan'ao Island [1].

Despite its many advantages, VSC-HVDC also has some drawbacks. One of the main drawbacks is the high cost, where the installation of VSCs and their control components is more expensive compared to LCC-HVDC, mainly due to the need for IGBT transistors and complex cooling systems [5]. In addition, VSC-HVDC can experience instability when connected to very weak AC networks due to difficulties in providing sufficient reactive power, which can cause voltage distortion and commutation failures [1],[4]. VSCs also have limitations on the voltage and power levels they can handle, which limits their use in certain applications [5]. Therefore, the use of better control than conventional PI control needs to be considered.

## **2. Comparison Performance Analysis of PI and PI-ANFIS in VSC-HVDC Transmission Systems**

### **2.1 Voltage Source Converter-High Voltage Direct Current**

VSC-HVDC operates by using converters consisting of electronically controllable IGBTs to turn electric current on and off. This allows the VSC to produce output voltage at the desired amplitude or phase angle [1]. The basic topology of a VSC-HVDC transmission system involves two AC terminals, one as a sender and the other

as a receiver, with VSCs at each terminal to convert and regulate DC and AC voltages [1]. The schematic in Figure 1. shows a VSC HVDC system where AC power is converted to DC by a VSC, transmitted over a DC link with smoothing components, and then converted back to AC by another VSC. The system includes resistors and inductors on both the AC and DC sides to represent their properties.

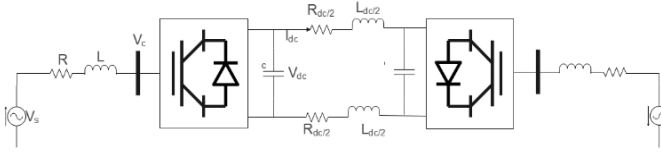


**Figure 1.** Schematic representation of VSC HVDC system

As explained in [6], the voltage equation in the dq domain for the terminal converter can be expressed as:

$$\begin{bmatrix} V_{sd} \\ V_{sq} \end{bmatrix} = R \begin{bmatrix} i_d \\ i_q \end{bmatrix} + L \frac{d}{dt} \begin{bmatrix} i_d \\ i_q \end{bmatrix} + \omega L \begin{bmatrix} -i_q \\ i_d \end{bmatrix} + \begin{bmatrix} V_{cd} \\ V_{cq} \end{bmatrix} \tag{1}$$

where  $V_{sd}$  is the source voltage component on the d axis and  $V_{sq}$  is the source voltage component on the q axis.  $i_d$  is the current component on the d axis and  $i_q$  is the current component on the q axis.  $R$  represents the total resistance of the transmission line and the filter.  $L$  represents the total inductance of the transmission line and the filter.  $\omega$  is the angular frequency of the AC grid.  $V_{cd}$  is the converter voltage on the d axis and  $V_{cq}$  is the converter voltage on the q axis. The orientation of the reference frame’s d-axis in alignment with the AC grid voltage vector results in the decomposition of voltage components into a constant d-axis component and a nullified q-axis component. Thus, the equations for AC active and reactive powers are expressed as follows:

$$P = \frac{3}{2} (V_{sd}i_d + V_{sq}i_q) = \frac{3}{2} (V_{sd}i_d) \tag{2}$$

$$P = \frac{3}{2} (V_{sq1}i_{d1} - V_{sd1}i_{q1}) = -\frac{3}{2} (V_{sd}i_q) \tag{3}$$

Assuming negligible power loss at the converter stations, the AC power equals the DC power, as expressed by:

$$P = P_{dc} = \frac{3}{2} (V_{sd}i_d) = V_{dc}i_{dc} \tag{4}$$

The dynamics of the can be expressed by:

$$i_{dc} = C \frac{dv_{dc}}{dt} + \frac{v_{dc}}{R_l} \tag{5}$$

where  $R_l$  represents the Thevenin equivalent resistance of the load as viewed from the VSC terminals, and  $C$  denotes the capacitance of the DC link.

Substituting (4) in (5), the  $v_{dc}$  dynamics can be written in terms of  $i_{dc}$  as they are in (6)

$$\left[ \frac{3}{2} \left( \frac{V_{sd}}{V_{dc}} \right) i_d = C \frac{dv_{dc}}{dt} \right] \quad (6)$$

Some of the main advantages of VSC-HVDC include operational flexibility, where VSC-HVDC can connect weak AC networks and even dead networks, as well as provide the necessary reactive power compensation without requiring synchronous generators [7],[3]. Better efficiency and control are also other advantages, as VSCs can independently control active and reactive power, which is very useful in the integration of renewable energy sources such as wind and solar that have fluctuating characteristics [3]. In addition, this technology requires less space and produces lower harmonics, which means it has a smaller environmental impact compared to other HVDC technologies [8].

## 2.2 Proportional-Integral Controller

PI (Proportional-Integral) controller is a controller method widely used in industrial control systems. This controller combines two main components: proportional control which produces an output proportional to the magnitude of the error, and integral control which produces an output based on the accumulated error over time [9]. The overall PI control equation can be expressed as:

$$u(t) = K_p \times e(t) + K_i \times \int e(t) dt \quad (7)$$

where  $u(t)$  is the control signal,  $K_p$  is the proportional gain,  $K_i$  is the integral gain, and  $e(t)$  is the error between the setpoint value and the actual value at time  $t$ .

In the application of PI control in VSC-HVDC transmission systems, the PI controller is used to regulate various variables such as current, voltage, active power, and reactive power. The PI controller can be employed in the current control loop to regulate currents in the d and q axes, in the DC voltage control loop to regulate DC voltage, as well as in the active power control loop and reactive power control loop to regulate the flow of active and reactive power. The selection of  $K_p$  and  $K_i$  parameters in the PI controller is crucial for achieving optimal system performance. The proportional gain ( $K_p$ ) affects the system's response speed to changes in the setpoint or disturbances, while the integral gain ( $K_i$ ) influences the system's ability to eliminate steady-state errors.

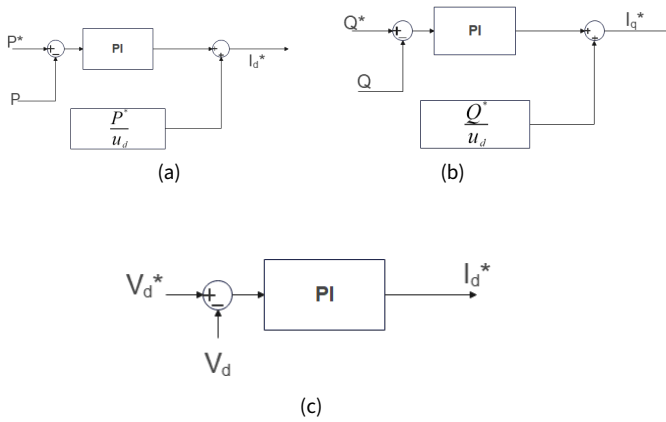


Figure 2. PI control in VSC-HVDC

Figure 2.a shows the PI controller for active power control, where  $P^*$  is the active power reference value,  $P$  is the measured active power,  $u_d$  is the d-axis voltage component in the dq reference frame, and  $I_d$  is the reference value for the d-axis current component. Figure 2.b illustrates the PI controller for reactive power control, where  $Q^*$  is the reactive power reference value,  $Q$  is the measured reactive power, and  $I_q$  is the reference value for the q-axis current component. Figure 2.c depicts the PI controller for DC voltage control, where  $V_d^*$  is the DC voltage reference value, and  $V_d$  is the measured DC voltage value.

The combination of these two components allows the PI controller to eliminate offset and accelerate system response [10]. Although PI controllers have many advantages, there are some limitations that need to be considered. One of the main limitations is the inability of PI controllers to handle large and rapid load disturbances [11]. This can cause overshoot and oscillation in the system response. In addition, PI controllers are also susceptible to integral wind-up phenomena, where the integral component continues to accumulate error even though the controller output has reached its maximum limit [12]. This phenomenon can slow down the system response and cause instability. Another limitation is the difficulty in tuning PI controller parameters, especially in complex or nonlinear systems [13]. Improper tuning can cause slow system response, oscillation, or even instability. Therefore, robust and adaptive tuning methods are needed to optimize the performance of PI controllers in various operating conditions [14].

### 2.3 Adaptive Neuro-Fuzzy Inference System

ANFIS is a hybrid intelligent system that combines the learning abilities of neural networks with the inference mechanism of fuzzy logic. This system offers a powerful framework for modeling complex systems and effectively handling non-linearity. The main advantage of ANFIS lies in its ability to combine human-like reasoning styles of fuzzy systems with the learning and adaptation capabilities of neural networks. One of the main applications of ANFIS is in fault location detection in VSC-HVDC systems. This hybrid approach utilizes an optimized neuro-fuzzy system to improve

the accuracy and efficiency of the fault detection mechanism, ensuring system reliability and stability [15]. In addition, ANFIS is also applied in VSC-HVDC systems to enhance black-start capability. The adaptive nature of ANFIS allows it to handle the complexity of power recovery after disturbances, ensuring a smoother and faster recovery process [16].

In multi-area hybrid power systems, ANFIS has been used to handle various resources, ensuring optimal stability and performance under various operating conditions. The integration of ANFIS with PID control strategies enhances the adaptability and robustness of such control systems [17]. Artificial intelligence-based control techniques for HVDC systems have also been widely explored using ANFIS. These techniques leverage the learning capabilities of ANFIS to optimize control strategies, resulting in improved performance in power transmission and stability under varying load conditions [18].

In medium voltage (MV) networks, ANFIS is used to protect Static Synchronous Series Compensators (SSSC). Using a combination of varistors and thyristors, the ANFIS controller improves system stability and protects the SSSC from voltage fluctuations caused by load variations [19],[20]. In renewable energy applications, ANFIS is used in grid-connected photovoltaic (PV) systems equipped with battery energy storage (BES). This controller ensures maximum power extraction, reactive power compensation, harmonic reduction, and smooth transitions between grid-connected and standalone modes [21].

Power quality improvement using a Unified Power Quality Conditioner (UPQC) incorporating a hysteresis-based ANFIS controller shows significant improvements in power quality. This system effectively reduces voltage sags, swells, and harmonics, ensuring consistent power delivery and enhancing the reliability of the power grid [22].

The main advantages of ANFIS include its high adaptability to changing conditions and new patterns, its ability to effectively handle uncertainty and non-linearity, and its capacity to integrate human-like reasoning with data-driven learning, enhancing the decision-making process. The application of ANFIS in various domains, particularly in power systems and renewable energy, highlights its flexibility and effectiveness. By harnessing the strengths of neural networks and fuzzy logic, ANFIS provides a powerful tool for modeling, control, and optimization tasks. This research further analyzes the potential of ANFIS in its application to VSC-HVDC controllers to improve the response of conventional PI control.

### 3. Research Methods

The research methods used in this paper are illustrated in Figure 3, which outlines the sequential flow of the research process. The figure details each step, beginning with data collection and theoretical foundation, followed by modeling the PI system. Next, it involves developing a PI-ANFIS model using the training data, and subsequently evaluating and refining this new model. The final step is drawing conclusions based on the analysis and improvements made throughout the research process.

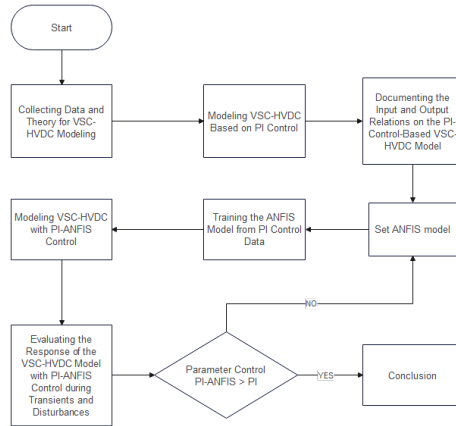


Figure 3. Research Flowchart

*Start & collecting data and theory:* The first step in this research is to collect relevant data and theories for modeling the VSC HVDC system. The collected data can include system parameters, configurations, and component characteristics. The studied theories include the working principles of VSC HVDC, PI control techniques, and ANFIS methods.

*Modeling VSC-HVDC based on PI control:* At this stage, the VSC-HVDC Model. This model is developed by considering system dynamics, control parameter settings, and desired performance criteria. The simulation software MATLAB/Simulink was used for modeling. After gathering the necessary data and theoretical background, the next step is to develop a model of the VSC-HVDC transmission system using PI control. The goal of this modeling is to create an accurate mathematical representation of the VSC-HVDC system, which will serve as the basis for analysis, simulation, and control design. This process involves deriving the dynamic equations that describe the behavior of the VSC converter, transformers, reactors, capacitors, and other components in the system. These equations can be derived using coordinate transformations with Park and Clarke transformations. Once the VSC-HVDC model is obtained, the next step is to integrate PI control into the model. The PI controller is used to regulate variables such as current, voltage, active power, and reactive power to follow desired reference values. The PI control parameters, such as  $K_p$  and  $K_i$  are determined based on desired performance criteria such as response time, overshoot, and steady-state error. The VSC-HVDC model with PI control is simulated using MATLAB Simulink. It consists of five main parts: Sending AC system (230 kV, 2000 MVA, 50 Hz) connected to an identical receiving AC system via VSC-HVDC transmission (200 MVA, +/- 100 kV). The VSC-HVDC transmission includes a rectifier terminal, transmission line, and inverter terminal.

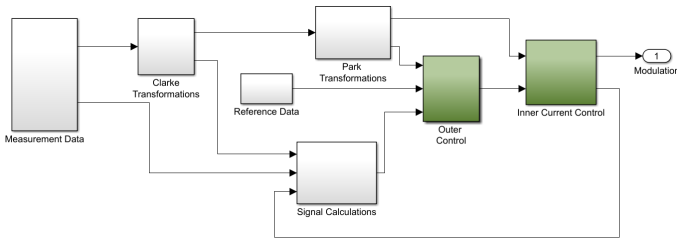


Figure 4. illustrates the VSC terminal simulation model.

The model from Figure 4 comprises several key sections described as follows. **Measurement Data**, This section inputs the necessary measurement data required for controlling the VSC transmission system. **Reference Data**, This section inputs the desired reference values for the system variables. **Clarke Transformation**, This section performs the Clarke transformation on the measured data before further processing. **Park Transformation**: After the Clarke transformation, the data is further processed using the Park transformation. **Signal Calculation**, this section calculates the necessary signals based on the transformed measurement data. Calculations include estimates of active power, reactive power, and other relevant variables for system control. **Outer Control**, This section regulates active power ( $K_p = 2$ ,  $K_i = 20$ ) and reactive power ( $K_p = 2$ ,  $K_i = 20$ ) at the rectifier terminal. It also controls DC voltage ( $K_p = 2$ ,  $K_i = 40$ ) and reactive power ( $K_p = 2$ ,  $K_i = 20$ ) at the rectifier terminal using PI control. The outer control generates reference current values for the inner current control process. **Inner Current Control**, this section processes the reference current values generated by the outer active-reactive power control. Current control ( $K_p = 0.6$ ;  $K_i = 6$ ) generates reference voltage values, which will be used to determine the switching modulation in the VSC converter. By combining these sections, the VSC terminal simulation model can accurately represent the operation of the HVDC transmission system. This model allows for the analysis of system performance under various operating conditions and the testing of different control strategies.

*Documenting input and output relationships on the PI control based VSC-HVDC model based on PI control*: After the VSC-HVDC model with PI control is developed, the next step is to identify and record the relationships between the system's inputs and outputs. These relationships are important for understanding the system's behavior and as a basis for developing the PI-ANFIS control.

*Set ANFIS model*: This step is a crucial phase in the development of the PI-ANFIS control system for VSC-HVDC. In this stage, the basic structure of the ANFIS to be used is determined. The ANFIS modeling process using the Neuro-Fuzzy Designer in MATLAB. The initiation of the Fuzzy Inference System (FIS) structure in ANFIS is carried out using the sub-clustering method to yield an optimal FIS structure. In the sub-clustering process within ANFIS, several important parameters need to be understood. The range of influence is a parameter that determines the extent of the area around each cluster center (centroid) that is influenced by the data during the clustering process. This parameter controls the size of the clusters formed; clusters with a large range of influence will encompass more data and become larger, whereas

clusters with a small range of influence will be more localized. In this study, the range of influence used is 0.5. The squash factor, on the other hand, adjusts how quickly the membership function of data in a cluster decreases as it moves away from the cluster center. This parameter controls the degree of fuzziness of the membership function within a cluster. A larger squash factor results in a slower decrease of the membership function, while a smaller squash factor leads to a faster decrease. In this study, the squash factor used is 1.25. The accept ratio is a threshold value used to decide whether certain data can be accepted into an existing cluster. This parameter controls how easily data is accepted into an existing cluster; a low accept ratio tends to result in more clusters because fewer data points are accepted into existing clusters, while a high accept ratio results in fewer clusters. In this study, the accept ratio used is 0.5. Finally, the reject ratio is a threshold value used to determine whether certain data is not accepted into an existing cluster and should be considered for the formation of a new cluster. The reject ratio controls how strict the criteria are for rejecting data from existing clusters; a low reject ratio means more data points are rejected from existing clusters, prompting the formation of more new clusters, while a high reject ratio means fewer data points are rejected, thereby reducing the number of new clusters formed. In this study, the reject ratio used is 0.15. By carefully selecting and tuning these parameters, the sub-clustering method in ANFIS can be optimized to create a robust and effective FIS structure, which is crucial for the accurate modeling and analysis of complex systems.

*Training the ANFIS model from PI control data:* The data obtained from the VSC-HVDC model with PI control is used to train the ANFIS model. This training process involves adjusting the ANFIS parameters until the model can accurately predict the system's output based on the given input.

*Modeling VSC-HVDC with PI-ANFIS control:* After successfully training the ANFIS model using the input-output relationship data from the PI control, the next step is to integrate the PI-ANFIS control into the VSC-HVDC model. The goal of this stage is to develop a comprehensive VSC-HVDC model with PI-ANFIS control, which will serve as the basis for analysis, simulation, and system performance evaluation. The use of PI-ANFIS in VSC-HVDC as utilized in this paper is based on [23], where the control block diagram is shown in Figure 5.

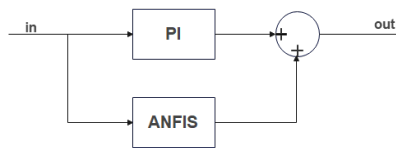


Figure 5. PI-ANFIS Control Model

Where *in* and *out* are the input and output of controller, respectively. *Evaluating the response of the VSC-HVDC model with PI-ANFIS control during transients and disturbances:* After the VSC-HVDC model with PI-ANFIS control is developed, the next step is to perform simulations to observe the system's response under transient conditions and during disturbances.

The parameters of reference are settling time, recovery time, overshoot, and undershoot during both transient and permanent disturbance conditions, which are then compared with the PI controller.

*Drawing conclusions:* The final step in this research is to draw conclusions based on the analysis and optimization results. The conclusions may include the effectiveness of PI-ANFIS control compared to PI control, improvements in VSC-HVDC system performance, as well as potential applications and further developments of the proposed method.

This research flow provides a systematic approach to modeling, analyzing, and optimizing the VSC-HVDC system using PI and PI-ANFIS control. The research results are expected to contribute to the development of more efficient, reliable, and stable power transmission systems.

## 4. Analysis of PI and PI-ANFIS in VSC-HVDC Transmission Systems

### 4.1 Transients

The use of PI-ANFIS control in the active and reactive power control system on the rectifier and inverter shows a significant performance improvement compared to the use of standard PI control. The following analysis will outline the advantages of using PI-ANFIS based on the provided data, highlighting its benefits in reducing overshoot and accelerating settling time.

#### 4.1.1 Active Power Control on Rectifiers

The comparison of active power controller performance between the PI and PI-ANFIS models during transient conditions at the rectifier terminal is illustrated in Figure 6. This figure highlights the differences in how each controller manages active power, providing insights into their relative effectiveness in handling transient states.

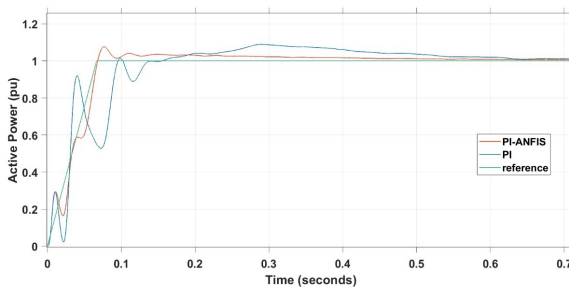


Figure 6. Comparison of active power with PI and PI-ANFIS control during transients on the rectifier side.

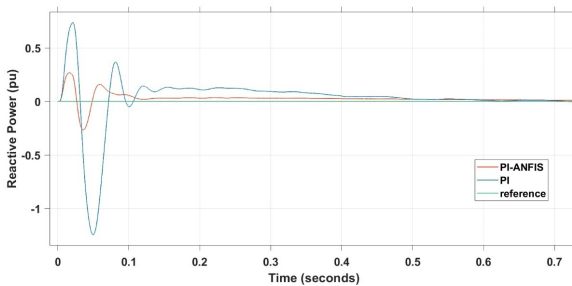
As shown in Figure 6 active power control on the rectifier, the use of PI-ANFIS can reduce the overshoot value from 1.089 pu to 1.077 pu. Although the difference seems small, this indicates PI-ANFIS's ability to optimize system stability better than conventional PI control. More significant is the reduction in settling time from 0.42 seconds to 0.084 seconds. This nearly fivefold acceleration in settling time shows that PI-ANFIS can control the system with a much faster response, which is crucial

in active power control applications requiring quick responses to maintain system efficiency and stability.

The reduction in overshoot, though slight, still demonstrates that PI-ANFIS can adapt more precisely to system dynamics. However, what stands out more is PI-ANFIS's ability to accelerate the settling time. This means the system can reach a stable condition more quickly, reducing the time spent in undesirable transient states, thereby enhancing the overall efficiency of the system.

#### 4.1.2 Reactive Power Control on Rectifiers

Figure 7 illustrates the comparison of reactive power controller performance between the PI and PI-ANFIS models during transient conditions at the rectifier terminal. This figure emphasizes the differences in reactive power management by each controller, offering insights into their respective effectiveness in handling transient states.



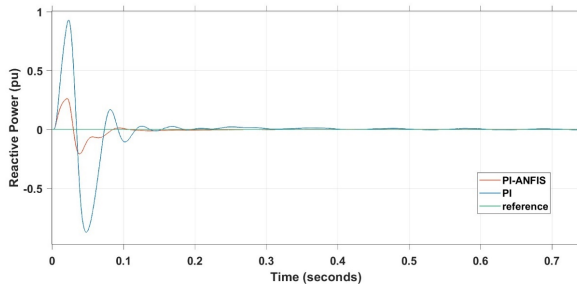
**Figure 7.** Comparison of reactive power with PI and PI-ANFIS control during transients on the rectifier side.

Figure 7 shows that in reactive power control on rectifiers, the use of PI-ANFIS shows exceptional capability in reducing overshoot values. The overshoot, which previously ranged from 0.737 pu to -1.244 pu, was successfully reduced to 0.268 pu to -0.267 pu. This significant reduction demonstrates that PI-ANFIS can more effectively control larger fluctuations. Settling time also decreased from 0.401 seconds to 0.103 seconds, accelerating the time for the system to reach a stable condition.

The reduction in overshoot from a substantial range to a smaller one shows that PI-ANFIS has a strong ability to adapt to load changes and operating conditions. Furthermore, the significant acceleration in settling time indicates that PI-ANFIS can make the system more responsive to dynamic changes, which is crucial in reactive power control applications that often experience sudden changes.

#### 4.1.3 Reactive Power Control on Inverters

Figure 8 showcases how the PI and PI-ANFIS models differ in managing reactive power at the inverter terminal during transient conditions. The illustration highlights the contrasting performance of these two reactive power control approaches.



**Figure 8.** Comparison of reactive power with PI and PI-ANFIS control during transients on the inverter side.

The result from Figure 8 show that on the inverter side, using PI-ANFIS in reactive power control shows a decrease in overshoot from a minimum value of  $-0.873$  pu and a maximum value of  $0.929$  pu to a minimum value of  $-0.207$  pu and a maximum value of  $0.263$  pu. Additionally, the settling time decreased from  $0.111$  seconds to  $0.074$  seconds. This reduction in overshoot and acceleration in settling time indicates that PI-ANFIS can significantly improve the responsiveness and stability of reactive power control on inverters.

The drastic reduction in overshoot in reactive power control on inverters shows that PI-ANFIS can manage reactive power transients more effectively. This is important for maintaining power quality and reducing the risk of equipment damage due to excessive power fluctuations. Additionally, further reduction in settling time shows that PI-ANFIS can provide a faster response, which is crucial for maintaining system stability under changing operational conditions.

#### 4.1.4 DC Voltage Control on Inverters

The performance results for the DC voltage controller from PI and PI-ANFIS can be observed in Figure 9.

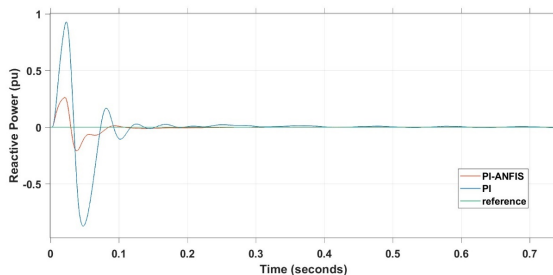


**Figure 9.** Comparison of DC voltage with PI and PI-ANFIS control during transients on the inverter side.

As Shown Figure 9 In DC voltage control, PI-ANFIS shows a reduction in overshoot from a value of  $1.455$  pu to  $1.267$  pu. Settling time also decreased from  $0.208$  seconds to  $0.169$  seconds. This indicates that PI-ANFIS can not only reduce large fluctuations but also accelerate the DC voltage stabilization process.

The ability of PI-ANFIS to reduce overshoot and accelerate settling time in DC voltage control shows that the control system can maintain more stable voltage in a shorter period. This is crucial for applications requiring high voltage stability and a quick response to load changes or disturbances. Reducing overshoot also helps reduce stress on system components, which can extend lifespan and improve overall system reliability.

All key points regarding the performance of PI and PI-ANFIS during transient conditions for each type of control are detailed in Table 1. The table highlights the performance differences and effectiveness of both control strategies. This comprehensive comparison provides insights into their behavior under transient conditions.

**Table 1.** Comparison of PI and PI-ANFIS control performance during transients.

	Controller		Settling time @0.95 pu (s)	Overshoot (pu)	Undershoot (pu)
	Rectifier	P	PI	0.420	1.077
PI-ANFIS			0.084	1.089	-
Q		PI	0.401	0.737	-1.244
		PI-ANFIS	0.103	0.268	-0.267
Inverter	Vdc	PI	0.208	1.455	-
		PI-ANFIS	0.169	1.267	-
	Q	PI	0.111	0.929	-0.873
		PI-ANFIS	0.074	-0.207	0.263

#### 4.2 During Permanent Disturbances

The results of the comparison between PI and PI-ANFIS control are shown in Figure 10 to Figure 13. These figures illustrate the differences in performance between the two control strategies. Each figure highlights specific aspects of their behavior under various conditions. The visual data provides a clear comparison, emphasizing the strengths and weaknesses of each approach. This detailed analysis helps to understand the effectiveness of PI and PI-ANFIS controllers.

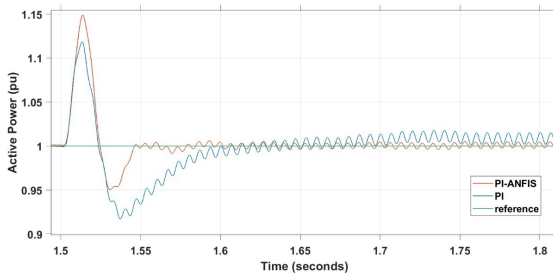


**Figure 10.** Comparison of active power with PI and PI-ANFIS control during permanent disturbances on the rectifier side.

The use of PI-ANFIS controllers in active power control on rectifiers shows exceptional capability in maintaining active power values close to the reference value. As shown Figure 10 Test results indicate that PI-ANFIS can keep the lowest active power point above 0.95 pu. This indicates a high level of stability and reliability in managing active power fluctuations, which is crucial in industrial applications where power disturbances are common.

Additionally, Figure 10 also shows that the recovery time experienced a significant improvement with the use of PI-ANFIS. Test results show that the recovery time decreased from 0.058 seconds with the PI controller to only 0.021 seconds with the PI-ANFIS controller, indicating an improvement of 0.037 seconds or 63.7%. This reduction in recovery time is essential as it accelerates the system's return to normal conditions after a disturbance, reducing the likelihood of damage and improving operational efficiency.

This performance improvement indicates that PI-ANFIS not only maintains active power stability but also significantly accelerates system response to disturbances. This provides significant advantages in operational contexts where quick recovery time and high reliability are priorities. Implementing PI-ANFIS can be an effective solution to enhance rectifier system performance in various industrial applications.

#### 4.2.1 Reactive Power Control on Rectifiers

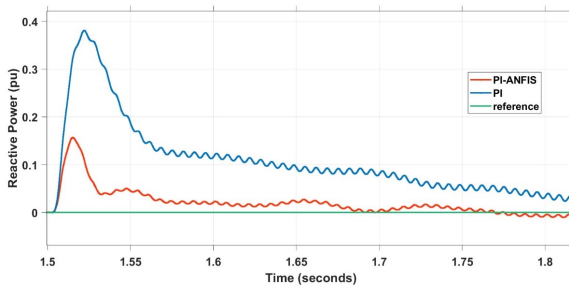


**Figure 11.** Comparison of reactive power with PI and PI-ANFIS control during permanent disturbances on the rectifier side.

In reactive power control on rectifiers, the use of PI-ANFIS shows clear improvement in maintaining reactive power stability. In Figure 11, the reactive power deviation from the reference value is significantly reduced from 0.381 pu with the PI controller to only 0.157 pu with the PI-ANFIS controller. This reduction in deviation reflects increased accuracy and precision in reactive power control, which is crucial in maintaining the quality of power consumed by loads.

Additionally, PI-ANFIS also demonstrates superiority in reducing recovery time after a disturbance. The PI controller requires up to 0.276 seconds to return to the reference value, whereas the PI-ANFIS controller only requires 0.03 seconds. This significant reduction in recovery time indicates that PI-ANFIS can respond to disturbances much more quickly and effectively, maintaining better continuity and power quality.

Overall, these results confirm that PI-ANFIS is a superior solution for reactive power control compared to conventional PI controllers. Its ability to reduce deviation and accelerate recovery time makes it an excellent choice for industrial applications requiring precise and responsive power control.

#### 4.2.2 Reactive Power Control on Inverters

Figure 12 compares the reactive power control response with PI and PI-ANFIS control during permanent disturbances on the inverter side. The graph plots reactive power (in per unit, pu) against time (in seconds). The performance of each control strategy is represented by different curves, showing how each controller handles the disturbance over time.

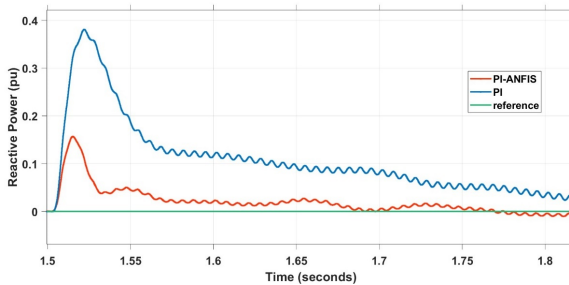


**Figure 12.** Comparison of reactive power with PI and PI-ANFIS control during permanent disturbances on the inverter side.

The comparison on the inverter's reactive power side can be seen in Figure 12. The PI-ANFIS control of reactive power shows significant performance improvement. Reactive power deviation after a disturbance decreased from 0.182 pu to only 0.066 pu. Reactive power deviation after a disturbance decreased from 0.182 pu to only 0.066 pu. This shows that PI-ANFIS can better control reactive power, reducing the impact of disturbances and maintaining higher power stability.

Additionally, the recovery time for reactive power control also shows significant improvement. The PI controller requires 0.069 seconds for recovery, while the PI-ANFIS controller only requires 0.018 seconds, or about 73% faster. This reduction in recovery time shows that PI-ANFIS can provide a quicker and more efficient response to disturbances, which is crucial for maintaining stable and reliable inverter operations.

Overall, the superior performance of PI-ANFIS in reactive power control on inverters confirms its potential as a more effective and efficient controller. This increased stability and responsiveness are highly valuable in industrial applications requiring high reliability and optimal power quality. Implementing PI-ANFIS in inverter systems can lead to significant performance improvements in the overall system.

### 4.2.3 DC Voltage Control on Inverters

Figure 13 compares the DC voltage response with PI and PI-ANFIS control during permanent disturbances on the inverter side. The graph plots DC Voltage power (in per unit, pu) against time (in seconds). The performance of each control strategy is represented by different curves, showing how each controller handles the disturbance over time

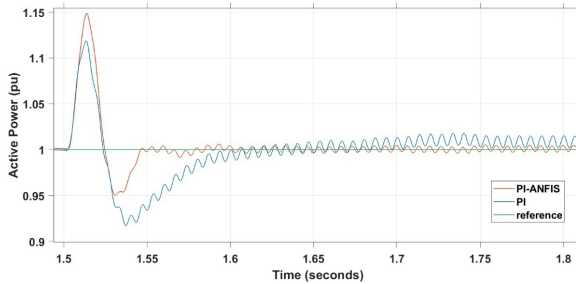


**Figure 13.** Comparison of DC voltage with PI and PI-ANFIS control during permanent disturbances on the inverter side.

In DC voltage control, Figure 13 demonstrates that while the PI-ANFIS controller exhibits a higher overshoot, the range between overshoot and undershoot is smaller, indicating improved performance compared to the PI controller. With PI-ANFIS, the DC voltage range is maintained between 1.090 pu and 0.846 pu, whereas the PI controller maintains it between 1.11 pu and 0.828 pu. This enhanced stability is crucial for ensuring consistent power quality and minimizing voltage fluctuations that could damage equipment.

Additionally, PI-ANFIS also shows improvement in recovery time. A reduction of 0.003 seconds or about 3.8% in recovery time indicates that PI-ANFIS can enhance the overall system response. Although this improvement is not as significant in power control, it still contributes positively to system reliability and operational efficiency.

Overall, the use of PI-ANFIS in DC voltage control on inverters shows significant benefits in terms of stability and responsiveness. Although the improvement is not as large in power control, this consistent improvement confirms PI-ANFIS's potential as a better solution in DC voltage control. Implementing PI-ANFIS can provide long-term benefits in terms of system reliability and reducing the risk of equipment damage due to voltage variations.

All key points from Figure 10 to Figure 13 are comprehensively summarized in Table 2. and Table 3. Table 2. highlights the recovery time and the improvements in recovery time for both the PI and PI-ANFIS systems. Table 3 provides a detailed comparison of the undershoot and overshoot values for the PI and PI-ANFIS systems, showcasing the differences in performance between these two control strategies. These tables collectively provide a clear and concise overview of the effectiveness and efficiency of the PI-ANFIS controller compared to the traditional PI controller in various aspects of reactive power and DC voltage control.

**Table 2.** Comparison of settling time and recovery time for PI and PI-ANFIS control during permanent disturbances.

Controller			Settling time (s)	Recovery time (s)		
				@0.95 pu	(s)	$\Delta$ (%)
Rectifier	P	PI	1.558	0.058	0.037	63.79
		PI-ANFIS	1.521	0.021		
	Q	PI	1.776	0.276	0.246	89.13
		PI-ANFIS	1.530	0.03		
Inverter	Vdc	PI	1.578	0.078	0.003	3.85
		PI-ANFIS	1.575	0.075		
	Q	PI	1.569	0.069	0.051	73.91
		PI-ANFIS	1.518	0.018		

**Table 3.** Comparison of undershoot and overshoot for PI and PI-ANFIS control during permanent disturbances.

Controller		Overshoot (pu)	Undershoot (pu)	Settling time (s)
P	PI	1.119	0.917	1.558
	PI-ANFIS	1.149	0.95	1.521
Q	PI	0.381	<0.01	1.776
	PI-ANFIS	0.157	<0.01	1.530
Vdc	PI	1.095	0.828	1.578
	PI-ANFIS	1.11	0.846	1.575
Q	PI	0.182	<0.01	1.569
	PI-ANFIS	0.066	<0.01	1.518

### 4.3 During Temporary Disturbances

During temporary disturbances, the performance of PI and PI-ANFIS controllers can be thoroughly analyzed from the results presented in Figures 14 to 17. These figures provide detailed insights into how each controller manages system stability and performance under transient conditions. By examining these results, we can compare the effectiveness of PI and PI-ANFIS in mitigating the impacts of disturbances and maintaining desired control parameters. This comprehensive analysis helps in understanding the strengths and weaknesses of each control strategy in handling temporary disruptions.

#### 4.3.1 Active Power Control on Rectifiers

Figure 14 compares the active power response with PI and PI-ANFIS control during permanent disturbances on the rectifier side. The graph plots active power (in per unit, pu) against time (in seconds). The performance of each control strategy is represented by different curves, showing how each controller handles the disturbance over time.

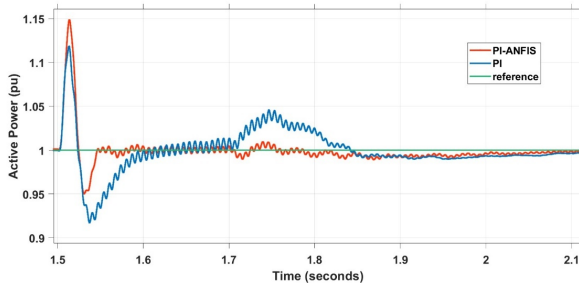


**Figure 14.** Comparison of active power with PI and PI-ANFIS control during permanent disturbances on the rectifier side.

The results obtained show that the VSC-HVDC system with PI-ANFIS control demonstrates significant superiority in recovery time and active power stability on rectifiers after disturbances. PI-ANFIS control accelerates the system recovery time to 0.021 seconds compared to 0.058 seconds with conventional PI control. This acceleration shows that PI-ANFIS can handle temporary disturbances more efficiently, which is crucial for maintaining the continuous operation of HVDC systems.

Additionally, PI-ANFIS control provides better active power stability. After the disturbance, the active power change with PI-ANFIS is below 0.01 pu, much lower than the 0.046 pu increase with PI control. Better power stability reduces potential stress on system components and improves operational reliability. This shows that PI-ANFIS control can maintain stable conditions with minimal power fluctuations, a significant advantage in HVDC system operations.

Finally, PI-ANFIS control shows higher accuracy and precision. The shorter time for active power to return to the reference value with PI-ANFIS compared to PI, namely 0.114 seconds, indicates more precise power regulation capability. This accuracy and precision are crucial in maintaining the efficiency and effectiveness of HVDC system operations, especially in disturbance scenarios. This overall analysis confirms that implementing PI-ANFIS control offers a superior solution for modern power systems, providing fast response, better stability, and high control accuracy.

#### 4.3.2 Reactive Power Control on Rectifiers

A detailed comparison of the reactive power response between PI and PI-ANFIS control strategies during temporary disturbances on the rectifier side is illustrated in Figure 15. The graph plots reactive power, measured in per unit (pu), against time in seconds. Various curves depict the performance of each control strategy, demonstrating how they manage disturbances over time. This visual representation allows for the observation of distinct performance characteristics between the PI

and PI-ANFIS controllers. The comparison highlights differences in reactive power stability and recovery times, offering valuable insights into the relative effectiveness of each controller under transient conditions.

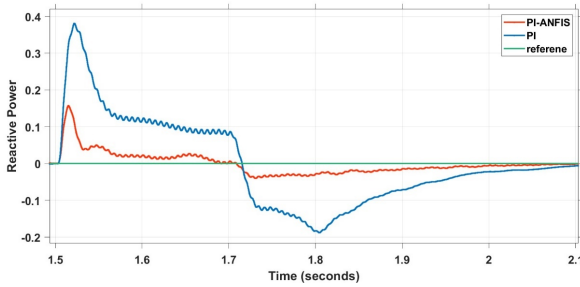


**Figure 15.** Comparison of reactive power with PI and PI-ANFIS control during permanent disturbances on the rectifier side.

This section compares the performance of the reactive power control system on rectifiers with PI and PI-ANFIS control on VSC-HVDC systems during temporary disturbances between 1.5 and 1.7 seconds. Figure 15 shows that PI control cannot stabilize reactive power before the disturbance disappears and can only achieve stability 0.233 seconds after the disturbance ends. In contrast, PI-ANFIS control shows better capability by achieving stability at 1.53 seconds, even before the disturbance completely disappears. This demonstrates the adaptive superiority and quick response of the PI-ANFIS system to temporary disturbances.

Besides response time, reactive power stability is also a crucial parameter in this analysis. PI-ANFIS control shows better performance in maintaining reactive power stability during and after disturbances. When the system transitions from monopole operation during disturbances to bipolar in normal conditions, there is no significant change in reactive power with PI-ANFIS control. Reactive power can be maintained within 0.05 pu of the reference value, with the highest deviation only 0.04 pu. This reflects PI-ANFIS's ability to maintain system stability under varying operating conditions.

In contrast, conventional PI control shows a larger deviation from the reference reactive power value when transitioning from monopole to bipolar operation. Reactive power deviation reaches up to 0.188 pu, indicating a lack of stability and responsiveness of PI control in facing significant operational changes. This instability can cause power system issues, such as increased power losses and potential damage to system components.

The superiority of PI-ANFIS in achieving faster stability and maintaining reactive power stability shows that PI-ANFIS can provide a more adaptive and responsive control solution for VSC-HVDC systems. The ability to achieve stability before the disturbance disappears indicates that PI-ANFIS can anticipate changes in system conditions more efficiently than PI control. Additionally, better reactive power stability reduces the risk of subsequent disturbances and increases system operational reliability.

### 4.3.3 Reactive Power Control on Inverters

A detailed comparison of the reactive power response between PI and PI-ANFIS control strategies during temporary disturbances on the inverter side is presented in Figure 16. The graph displays reactive power, measured in per unit (pu), plotted against time in seconds. Different curves represent the performance of each control strategy, showing how each controller manages the disturbance over time. This visual representation allows for the observation of distinct performance characteristics of the PI and PI-ANFIS controllers. The comparison highlights differences in reactive power stability and recovery times, providing valuable insights into the relative effectiveness of each controller under transient conditions.

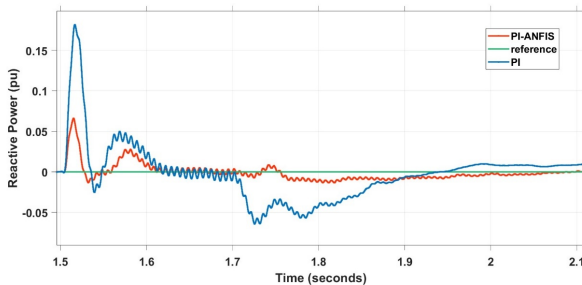


**Figure 16.** Comparison of reactive power with PI and PI-ANFIS control during permanent disturbances on the inverter side.

This section analyzes the performance of the reactive power control system on inverters using PI and PI-ANFIS control on VSC-HVDC systems during temporary disturbances between 1.5 and 1.7 seconds. Figure 16 shows that PI control takes longer to stabilize reactive power before the disturbance ends, with stabilization time reaching 0.069 seconds after the disturbance occurs. In contrast, PI-ANFIS control shows superior capability by achieving stability within 0.018 seconds after the disturbance occurs. The higher response speed of PI-ANFIS indicates significant potential in power control system applications requiring quick adjustments to dynamic conditions.

After the disturbance disappears and the system returns to normal operation with power transfer using a bipolar system (which uses a monopolar system during disturbances), there is a change in reactive power response. In PI control, reactive power decreases to  $-0.064$  pu, exceeding the stability limit of  $0.05$  pu. PI control then stabilizes the system  $0.092$  seconds after the disturbance ends. In contrast, PI-ANFIS control shows better performance in maintaining reactive power stability during and after disturbances. When the system transitions from monopolar operation during disturbances to bipolar in normal conditions, there is no significant change in reactive power with PI-ANFIS control. Reactive power can be maintained within  $0.05$  pu of the reference value, with the highest deviation only  $0.013$  pu.

This reflects PI-ANFIS's ability to maintain system stability under varying operating conditions, demonstrating the adaptive superiority and quick response of the PI-ANFIS system to temporary disturbances. The superiority of PI-ANFIS in achiev-

ing faster stability and maintaining reactive power stability shows that PI-ANFIS can provide a more adaptive and responsive control solution for VSC-HVDC systems. The ability to achieve stability before the disturbance ends indicates that PI-ANFIS can anticipate changes in system conditions more efficiently than PI control. Additionally, better reactive power stability reduces the risk of subsequent disturbances and increases system operational reliability.

From a technical perspective, the success of PI-ANFIS in maintaining reactive power stability within desired limits is closely related to the adaptive mechanisms implemented in the ANFIS algorithm. ANFIS, an adaptive inference system based on fuzzy logic, allows the system to learn and adapt to changing conditions quickly. This is a significant advantage over conventional PI control, which relies on fixed parameters and may not be responsive enough to unexpected disturbances. Therefore, integrating ANFIS into the PI control system provides additional flexibility that is highly needed in increasingly complex modern electrical applications.

#### 4.3.4 DC Voltage Control on Inverters

Figure 17 presents a comparison of the DC Voltage response between PI and PI-ANFIS control during temporary disturbances on the inverter side. The graph displays DC Voltage (in per unit, pu) plotted against time (in seconds). Different curves represent the performance of each control strategy, illustrating how each controller manages the disturbance over time.

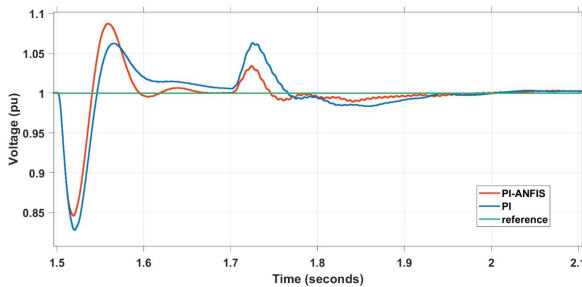


**Figure 17.** Comparison of DC voltage with PI and PI-ANFIS control during permanent disturbances on the inverter side.

This section discusses the performance of the DC voltage control system on inverters using PI and PI-ANFIS control on VSC-HVDC systems during temporary disturbances between 1.5 and 1.7 seconds. The result from Figure 17 shows that PI control takes longer to stabilize DC voltage before the disturbance ends, with stabilization time reaching 0.078 seconds after the disturbance occurs. In contrast, PI-ANFIS control shows better capability by achieving stability within 0.075 seconds after the disturbance occurs. The higher response speed of PI-ANFIS indicates significant potential in power control system applications requiring quick adjustments to dynamic conditions.

After the disturbance disappears and the system returns to normal operation with power transfer using a bipolar system (which uses a monopolar system during disturbances), there is a change in DC voltage response. In PI control, DC voltage increases up to 0.063 pu above the reference value, exceeding the stability limit of 0.05 pu. PI control then stabilizes the system 0.038 seconds after the disturbance ends. In contrast, PI-ANFIS control shows better performance in maintaining DC voltage stability during and after disturbances. When the system transitions from monopolar operation during disturbances to bipolar in normal conditions, there is no significant change in DC voltage with PI-ANFIS control. DC voltage can be maintained within 0.05 pu of the reference value, with the highest deviation only 0.034 pu.

This reflects PI-ANFIS's ability to maintain system stability under varying operating conditions, demonstrating the adaptive superiority and quick response of the PI-ANFIS system to temporary disturbances. The superiority of PI-ANFIS in achieving faster stability and maintaining DC voltage stability shows that PI-ANFIS can provide a more adaptive and responsive control solution for VSC-HVDC systems. The ability to achieve stability before the disturbance ends indicates that PI-ANFIS can anticipate changes in system conditions more efficiently than PI control. Additionally, better DC voltage stability reduces the risk of subsequent disturbances and increases system operational reliability.

From a technical perspective, the success of PI-ANFIS in maintaining DC voltage stability within desired limits is closely related to the adaptive mechanisms implemented in the ANFIS algorithm. ANFIS, an adaptive inference system based on fuzzy logic, allows the system to learn and adapt to changing conditions quickly. This is a significant advantage over conventional PI control, which relies on fixed parameters and may not be responsive enough to unexpected disturbances. Therefore, integrating ANFIS into the PI control system provides additional flexibility that is highly needed in increasingly complex modern electrical applications.

All key points from Figure 14 to Figure 17 are comprehensively summarized in Table 4. and Table 5. Table 2. highlights respond PI and PI-ANFIS control during temporary disturbances at the time fault occurrence. Show key point of the settling time and overshoot of the system. Table 3 provides a detailed comparison of PI and PI-ANFIS control response after disturbance, when system back to normal, showcasing the differences in performance between these two control strategies. These tables collectively provide a clear and concise overview of the effectiveness and efficiency of the PI-ANFIS controller compared to the traditional PI controller in various aspects of reactive power and DC voltage control.

**Table 4.** Comparison of PI and PI-ANFIS control response during temporary disturbances.

Controller			At fault occurrence	
			Settling time	Overshoot
Rectifier	P	PI	1.558	1.119
		PI-ANFIS	1.521	1.149
	Q	PI	1.776	0.381
		PI-ANFIS	1.530	0.157
Inverter	Vdc	PI	1.578	1.095
		PI-ANFIS	1.575	1.110
	Q	PI	1.569	0.182
		PI-ANFIS	1.518	0.066

**Table 5.** Comparison of PI and PI-ANFIS control response after disturbances.

Controller			After fault occurrence		
			Overshoot (pu)	Undershoot (pu)	Recovery time (s)
Rectifier	P	PI	1.046	<0.01	-
		PI-ANFIS	<0.01	<0.01	-
	Q	PI	0.085	-0.188	1.933
		PI-ANFIS	<0.01	-0.040	-
Inverter	Vdc	PI	1.063	0.983	1.738
		PI-ANFIS	1.034	0.989	-
	Q	PI	<0.01	-0.064	1.792
		PI-ANFIS	<0.01	-0.013	-

### 5. Conclusion

Based on the research and analysis conducted, several conclusions can be drawn. The use of PI-ANFIS control in VSC-HVDC transmission systems has proven to significantly improve system performance compared to conventional PI control, both under transient conditions and during disturbances. Under transient conditions, PI-ANFIS control can reduce overshoot values and accelerate the settling time for active power, reactive power, and DC voltage control on both the rectifier and inverter sides. This demonstrates PI-ANFIS’s ability to enhance system stability and responsiveness. During permanent disturbances, PI-ANFIS control shows better performance in maintaining the stability of active power, reactive power, and DC voltage. PI-ANFIS can reduce deviations from the reference values and speed up the system recovery time after disturbances compared to conventional PI control. In the case of temporary disturbances, PI-ANFIS control can achieve faster stability and maintain the stability of active power, reactive power, and DC voltage within the desired limits. PI-ANFIS also demonstrates better adaptability to changing operating conditions, such as transitions from monopolar to bipolar modes. The advantages of PI-ANFIS control in improving the performance of VSC-HVDC transmission systems are based on the adaptive and

learning capabilities of the ANFIS algorithm. Integrating ANFIS into PI control provides the additional flexibility needed to handle dynamic conditions and unexpected disturbances in the system.

## References

- [1] Y. Li et al. "Engineering Practices for the Integration of Large-Scale Renewable Energy VSC-HVDC Systems". In: *Global Energy Interconnection* 3.2 (2020), pp. 149–157. doi: 10.1016/j.gloi.2020.05.007.
- [2] M. A. Hannan et al. "Advanced Control Strategies of VSC Based HVDC Transmission System: Issues and Potential Recommendations". In: *IEEE Access* 6 (2018), pp. 78352–78369. doi: 10.1109/ACCESS.2018.2885010.
- [3] R. S. Garciarivas et al. "VSC-HVDC and Its Applications for Black Start Restoration Processes". In: *Applied Sciences (Switzerland)* 11.12 (2021), p. 5648. doi: 10.3390/app11125648.
- [4] H. Zhou et al. "Inductive Fault Current Limiters in VSC-HVDC Systems: A Review". In: *IEEE Access* 8 (2020), pp. 38185–38197. doi: 10.1109/ACCESS.2020.2976116.
- [5] H. Zheng et al. "Large-Signal Stability Analysis of DC Side of VSC-HVDC System Based on Estimation of Domain of Attraction". In: *IEEE Transactions on Power Systems* 37.5 (2022), pp. 3630–3641. doi: 10.1109/TPWRS.2022.3144336.
- [6] S. F. Faisal, A. R. Beig, and S. Thomas. "Real-time Implementation of Robust Loop-shaping Controller for a VSC HVDC System". In: *Energies* 14.16 (2021). doi: 10.3390/en14164955.
- [7] S. Huang et al. "Adaptive Droop-Based Hierarchical Optimal Voltage Control Scheme for VSC-HVdc Connected Offshore Wind Farm". In: *IEEE Transactions on Industrial Informatics* 17.12 (2021), pp. 8165–8176. doi: 10.1109/TII.2021.3065375.
- [8] K. Sun et al. "VSC-HVDC Inerties for Urban Power Grid Enhancement". In: *IEEE Transactions on Power Systems* 36.5 (2021), pp. 4745–4753. doi: 10.1109/TPWRS.2021.3067199.
- [9] K. J. Åström and T. Häggglund. *PID Controllers: Theory, Design, and Tuning*. Instrument Society of America, 1995.
- [10] Kiam Heong Ang, G. Chong, and Yun Li. "PID Control System Analysis, Design, and Technology". In: *IEEE Transactions on Control Systems Technology* 13.4 (2005), pp. 559–576.
- [11] A. Visioli. *Practical PID Control*. Springer Science & Business Media, 2006.
- [12] C. Bohn and D. P. Atherton. "An Analysis Package Comparing PID Anti-Windup Strategies". In: *IEEE Control Systems Magazine* 15.2 (2006), pp. 34–40.
- [13] K. J. Åström and T. Häggglund. "Revisiting the Ziegler–Nichols Step Response Method for PID Control". In: *Journal of Process Control* 14.6 (2004), pp. 635–650.
- [14] K. H. Ang, G. C. Chong, and Y. Li. "Relay Auto-Tuning of PID Controllers Using Iterative Feedback Tuning". In: *Journal of Process Control* 16.10 (2006), pp. 1069–1081.
- [15] R. Rohani and A. Koochaki. "A Hybrid Method Based on Optimized Neuro-Fuzzy System and Effective Features for Fault Location in VSC-HVDC Systems". In: *IEEE Access* 8 (2020), pp. 70861–70869. doi: 10.1109/ACCESS.2020.2986919.
- [16] P. Jyothsna, J. Deleep Kumar, and A. Professor. "Adaptive Fuzzy Logic Control with PI Strategies for VSC Based HVDC Transmission Systems to Improve Black-Start Capability". In: *NeuroQuantology* 20 (2022). doi: 10.48047/nq.2022.20.11.NQ66844.
- [17] B. Singh and S. Krishan Bishnoi. "An Application of ANFIS-PID Controller for Multi Area Hybrid Power System". In: *Artificial Intelligence and Communication Technologies*. Soft Computing Research Society, 2023, pp. 613–627. doi: 10.52458/978-81-955020-5-9-59.
- [18] H. Abdulwahid. "Artificial Intelligence-based Control Techniques for HVDC Systems". In: *Emerging Science Journal* 7.2 (Apr. 2023), pp. 643–653. doi: 10.28991/ESJ-2023-07-02-024.
- [19] N. Gurudeesh and K. Venkatapathi. "Design and Implementation of an ANFIS Controller for SSSC Protection in MV Network by using a Varistor and Thyristors". In: *International Journal of Scientific Research in Science and Technology* 11.3 (May 2024), pp. 340–346. doi: 10.32628/IJSRST.

- [20] V. V. Harini and M. Ramu. "Design and Analysis of ANFIS Controller Based Multi-functional VSC for Grid Connected Solar PV-BES System". In: *International Journal of Scientific Research in Science and Technology* 11.3 (May 2024), pp. 340–346. DOI: 10.32628/IJSRST.
- [21] R. Manivasagam and R. Prabakaran. "Power Quality Improvement by UPQC Using ANFIS-Based Hysteresis Controller". In: *Int. J. Operational Research* 37.2 (2020), pp. 174–197.
- [22] M. Ahmadi Kamarposhti *et al.* "Optimal Designing of Fuzzy-PID Controller in the Load-Frequency Control Loop of Hydro-Thermal Power System Connected to Wind Farm by HVDC Lines". In: *IEEE Access* 10 (2022), pp. 63812–63822. DOI: 10.1109/ACCESS.2022.3183155.
- [23] I. Made Ginarsa *et al.* "Strategy to Reduce Transient Current of Inverter-Side on an Average Value Model High Voltage Direct Current Using Adaptive Neuro-Fuzzy Inference System Controller". In: *International Journal of Electrical and Computer Engineering* 12.5 (Oct. 2022), pp. 4790–4800. DOI: 10.11591/ijece.v12i5.pp4790-4800.